Proceedings of the ASME 2012 6th International Conference on Energy Sustainability & 10th Fuel Cell Science, Engineering and Technology Conference
ESFuelCell2012
July 23-26, 2012, San Diego, CA, USA

ESFuelCell2012-91160

A STATISTICALLY BASED THERMAL CONDUCTIVITY MODEL FOR PEMFC GAS DIFFUSION LAYERS

Hamidreza Sadeghifar
PhD candidate
Mechatronic Systems Engineering,
School of Engineering Science,
Simon Fraser University,
Surrey V3T 0A3, BC, Canada
hamidreza_sadeghifar@sfu.ca

Majid Bahrami *
Associate Professor
Mechatronic Systems Engineering,
School of Engineering Science,
Simon Fraser University,
Surrey V3T 0A3, BC, Canada
mbahrami@sfu.ca

Ned Djilali
Professor
Department of Mechanical Engineering,
University of Victoria,
Victoria V8W 3P6, BC, Canada
ndjilali@uvic.ca

ABSTRACT

little attention has been paid to the geometrical parameters of Gas Diffusion Layers (GDLs), as many researchers have reported the GDL transport properties, like thermal conductivity, as a function of only one parameter; porosity. In this paper, a statistical unit cell approach is presented for estimation of the thermal conductivity on the basis of measured geometrical data such as the angles and also the distance between fibers (aspect ratio) and fiber diameter. The dependency of the thermal conductivity on each of these parameters is considered to obtain the best GDL structure. It is discussed, for the first time in this paper, that the parameter of the aspect ratio can usually be as important as porosity, and the traditional thought that a porous media with higher porosity has a lower thermal conductivity cannot always be correct. It is also concluded that the maximum thermal conductivity of a GDL is not a function of the aspect ratio and fiber diameter and only dependent on porosity and fiber angle. In general, the geometrical concepts and the optically measured data presented in this paper can be employed for estimation of other GDL transport properties such as permeability.

KEY WORDS:
Fibrous porous media, gas diffusion layer, thermal conductivity, fuel cell, aspect ratio

INTRODUCTION

Over the past few decades, there has been an increasing interest in the use of Proton Exchange Membrane Fuel Cells (PEMFCs) as an environmentally friendly power source. Accurate estimation of the temperature distribution and associated heat transfer rates in PEMFCs is essential to determine various transport phenomena such as water and species transport, reaction kinetics, and rate of phase change [1-3]. A key thermo-physical property for such purpose is the thermal conductivity of the membrane-electrode assembly components, particularly Gas Diffusion Layer (GDL) [4-7]. However, estimation of this property has been considered a risky endeavor for at least two main reasons. First due to lack of a deep understanding of the way that heat is transferred in such random micro-structured porous materials, and second, due to determination of geometrical parameters specific to each type of GDL. Meanwhile, along with the progress of the PEMFC technology, new GDLs with greatly different materials and characteristics are being manufactured for new and different applications. As a result, measurement of the geometrical characteristics of GDLs and developing a general model for prediction of their thermal conductivity at different operating conditions is essential for the modeling and design of PEMFCs.

A few models have been presented in the open literature for estimation of the through-plane thermal conductivity of GDLs. However, most of these approaches are based on only porosity and do not consider other important geometrical parameters such as fiber angles and aspect ratio, that is, the

ratio of the distance between fibers in the x and y directions. In these approaches [8-10], it has been typically tried to make a porous structure with the same porosity as the considered GDL and then, using some theoretical and governing equations, the thermal conductivity was calculated on the basis of the solid and pore fractions, i.e., porosity. As a result, the reported approaches in such studies give the same value for thermal conductivity of different GDLs with the same porosity, and usually overestimate [8] or underestimate [9-10] the measured thermal conductivity. Considering the structure of a fibrous porous media, it seems that the distance and also the angle between fibers can be important in heat transfer, and should be considered as well. Hence, we aim to develop a new analytical model that includes all the salient geometrical parameters.

Following the unit cell approach of Bahrami *et al.* [11] (also see [12-16]) that was applied successfully to several heat transfer applications such as packed beds, Sadeghi *et. al.* [1] developed a unit cell model for a fibrous porous media that can represent the structure of GDL. It was the first model that took the main geometrical parameters into account; however, Sadeghi *et al.* model [1] did not account for other GDL geometric parameters such as aspect ratio and fiber angles.

The focus of the present study will mainly be on determination of the geometrical parameters of different GDLs and applying them to a statistical unit dell approach. A comprehensive parametric study on these parameters is performed to investigate their effects on heat transfer and determine the most dominant parameters. The results of this study can provide detailed information on the thermal conductivity of various types of GDLs useful for performance modeling and also guidelines and insight for GDL manufacturers.

NOMENCLATURE

AR	aspect ratio
a,b	major and minor semi axes of elliptical contact, m
a,b	upper and lower integral bonds (variable p)
c	constant
d	fiber diameter, m
$d_{p,ave}$	average pore diameter, m
E	Young's modulus, Pa
E'	effective elastic modulus, Pa
Exp.	experimental value
F(p)	statistical distribution function of variable p
F_1	integral function of $(\rho'\rho''^{-1})$
F_{max}	maximum force on each contact point, N
GDL	Gas Diffusion Layer
k_{eff}	effective thermal conductivity, $Wm^{-1} K^{-1}$
l	distance between two fibers in the x direction, m
M	arbitrary quantity
MIP	Mercury Intrusion Porosimetry
MPL	Micro Porous Layer
M_g	gas molecular weight, g mol^{-1}
M_s	solid molecular weight, g mol^{-1}
N	number of data
N_A	number of the measured areas between fibers
P	probability
PDF	probability density function
PTFE	Polytetrafluoroethylene
p	random variable (deviation from the average value)
P_{GDL}	GDL pressure, Pa
Pr	Prandtl number
R	Thermal resistance, KW^{-1}
R_{co}	constriction resistance, KW^{-1}
R_{sp}	spreading resistance, KW^{-1}
R^*	thermal resistance correction factor
T	Temperature, K
w	distance between two fibers in the y direction, m

Greek letter

α	thermal accommodation parameter
μ	mean (Gaussian distribution)
β	fluid property parameter
γ	heat capacity ratio
ε	porosity
η	modulus of elliptic integral
θ	angle between two fibers, Rad
$\bar{\theta}$	average value of the measured angles, Rad
λ	ratio of relative radii of curvature $(\rho'\rho''^{-1})$
ρ', ρ''	major and minor relative radii of curvature, m
σ	standard deviation (Gaussian distribution)
υ	Poisson's ratio
Λ	mean free path of gas molecules, m
s	solid (carbon fiber)

Subscript

1	bottom block of the unit cell
2	top block of the unit cell
∞	standard condition state
ave	average value
cor	corrected value
eff	effective (overall) value
g	gas
gc	gas filled gap
i	i-th component of a set of variables or summation index
m	measured
max	maximum value
ref	reference value
tot	total

Superscript

*	correction factor.

2. MODEL DEVELOPMENT AND GEOMETRICAL DATA MEASUREMENTS

The temperature field and heat transfer rates in a fibrous porous media depend on a variety of factors including geometrical, material, mechanical, and thermal properties, as well as operating conditions. As mentioned, the structure of GDLs is anisotropic, so is its thermal conductivity, and thus, the geometrical modelling will be important. Here we focus on modeling of the through-plane thermal conductivity, though the presented concept is general and, with minor modifications, can be used for estimation of other transport properties such as in-plane thermal conductivity and permeability. In general, the present model is an extension of the model of Sadeghi *et. al.* [1], which relies on unit cell approach considering the GDL as a periodic fibrous micro structure, and assumes:

(1) 3-D repeating basic cell
(2) Steady state one-dimensional heat transfer
(3) Negligible natural convection within the basic cell
(4) No radiation heat transfer between the neighboring fibres

In addition to the above assumptions, we can also consider some additional features, as improvements, to make the model closer to the reality of a GDL structure:

(5) The statistical distribution of the angles between fibers in two adjacent layers: the average value of the angles and their deviations from the average value
(6) Employing true value of aspect ratio for various GDL types
(7) The statistical distribution of the fiber diameters.

Our aim in this study is to present a statistical unit cell approach by modifying the Sadeghi *et al*. model from the geometrical modelling viewpoint to extend its applicability to a broader range of GDL types, as well as to investigate the significant effects of geometrical parameters on thermal conductivity, which has not been considered in the literature so far. Detail development of the Sadeghei's model can be found elsewhere [1] and here we will focus on the improvements to that model. In fact, the main focus will be on how to measure or determine the geometrical parameters of each GDL, and then, how to implement them to the unit cell model.

In general, the unit cell models are based on one basic cell repeated throughout the whole media, which will be a representative of that media [1,11]. In the case of a fibrous porous media with parallel fibers in each layer, such as the most types of GDLs, a simple, still comprehensive, geometrical model like the one shown in Fig. 1, seems to be useful. In this figure, l and w are the distance between fibers in the x and y directions, d the fiber diameter, and θ the angle between fibers in two adjacent layers, respectively. The porosity (ε) of the unit cell will be a function of all these geometrical parameters, as given by [1]:

$$\varepsilon = 1 - \frac{\pi d}{8}\left(\frac{l+\frac{w}{\cos(\theta)}}{lw}\right) \qquad (1)$$

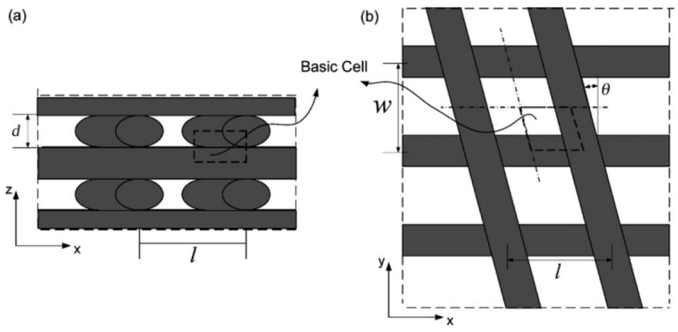

Fig. 1: Front view (a) and top view (b) of the geometrical model of GDL [1]

In principal, the unit cell model consists of mechanical and thermal models [1,11-16] applied to the defined unit cell [1,11]. Ultimately, using Fourier's law of heat conduction and total thermal resistance network concept, the effective thermal conductivity can be obtained (k_{eff}) as a function of geometrical parameters, i.e., $k_{\text{eff}} = f(\varepsilon, \theta, d, l, w)$. The thermal resistance network for the unit cell consisting of the top and bottom blocks is represented in Fig. 2. All the equations of the unit cell model are listed in Table 1.

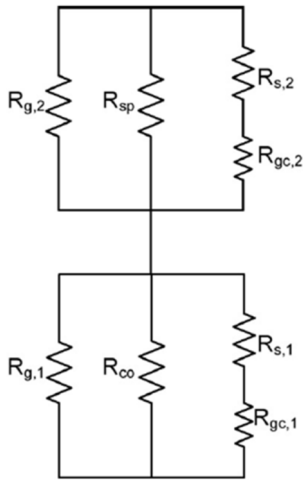

Fig. 2: Thermal resistance network for the top and bottom blocks of the unit cell [1]

Table 1: Equations of the unit cell model

Parameter	Equation	Number
Minor relative radii of contact curvature	$\rho'' = \frac{d}{\sqrt{2(1-\cos(2\theta))+2}}$	(2)
Major relative radii of contact curvature	$\rho' = \frac{1}{(4/d - 1/\rho'')}$	(3)
Integral function of $(\rho'\rho''^{-1})$	$F_1 = \frac{19.1\sqrt{\lambda}}{1+16.76\sqrt{\lambda}+1.34\lambda}$, $\lambda = \rho'/\rho''$	(4-5)
Maximum force on each contact point	$F_{max} = \frac{P_{GDL} lw}{4}$	(6)
Effective elastic modulus	$E' = (\frac{1-v_1^2}{E_1} + \frac{1-v_2^2}{E_2})^{-1}$	(7)
Major semi axis of elliptical contact	$a = b\,(\frac{\rho'}{\rho''})^{2/3}$	(8)
Minor semi axis of elliptical contact	$b = (\frac{\rho''}{\rho'} \frac{3F\sqrt{\rho'\rho''}}{4E'})^{1/3} F_1$	(9)
Solid thermal accommodation parameter	$\alpha_s = \exp\left[-0.57\left(\frac{T_s-273}{273}\right)\right](\frac{1.4M_g}{6.8+1.4M_g}) + \frac{2.4\left(\frac{M_g}{M_s}\right)}{\left(1+\frac{M_g}{M_s}\right)^2} \times \left\{1 - \exp\left[-0.57\left(\frac{T_s-273}{273}\right)\right]\right\}$	(10)
Thermal accommodation parameter	$\alpha = \left(\frac{2-\alpha_s}{\alpha_s}\right) + 1$	(11)
Fluid property parameter	$\beta = \frac{2\gamma}{Pr(\gamma+1)}$	(12)
Mean free path of gas molecules	$\Lambda = \Lambda_{g,\infty}(\frac{T_g}{T_{g,\infty}})(\frac{P_{g,\infty}}{P_g})$	(13)
Gas thermal resistance of bottom block	$\frac{1}{R_{g,1}} = k_g(\frac{l(w-\frac{d}{2})}{2(\frac{d}{2}+\alpha\beta\gamma)})$	(14)
Gas filled gap thermal resistance of bottom block	$\frac{1}{R_{gc,1}} = k_g\left(\frac{l}{2}\right)(\frac{2\alpha\beta\gamma}{\sqrt{(\alpha\beta\gamma)^2-1}}\ tan^{-1}(\sqrt{\frac{\alpha\beta\gamma+1}{\alpha\beta\gamma-1}}))$	(15)
Gas thermal resistance of top block	$\frac{1}{R_{g,2}} = k_g(\frac{w}{2})\frac{(\frac{l}{2}-\frac{d/2}{\cos(\theta)})}{d/2+\alpha\beta\gamma}$	(16)
Gas filled gap thermal resistance of top block	$\frac{1}{R_{gc,2}} = \frac{k_g\left(\frac{w}{2}\right)}{\cos(\theta)}(\frac{2\alpha\beta\gamma}{\sqrt{(\alpha\beta\gamma)^2-1}}\ tan^{-1}(\sqrt{\frac{\alpha\beta\gamma+1}{\alpha\beta\gamma-1}}))$	(17)
Spreading/constriction resistance & modulus of elliptic integral	$R_{sp}\ or\ R_{co} = \frac{1}{2\pi ka}\int_0^{\frac{\pi}{2}} \frac{dt}{\sqrt{1-\eta^2 sin^2 t}}$, $\eta = \frac{1}{\sqrt{1-(b/a)^2}}$	(18-19)
Total thermal Resistance	$R_{tot} = \left[\frac{1}{R_{g,1}} + \frac{1}{R_{gc,1}} + \frac{1}{R_{co}}\right]^{-1} + \left[\frac{1}{R_{g,2}} + \frac{1}{R_{gc,2}} + \frac{1}{R_{sp}}\right]^{-1}$	(20)
Effective thermal conductivity	$k_{\text{eff}} = \frac{4d}{lwR_{tot}}$	(21)

2-1. Measurement of geometrical parameters

Fibrous porous media such as GDLs can be different in structure and geometry by having different angle distribution, aspect ratio, and fiber diameter. Even these parameters can be distinct for the two porous media with the same porosity. For instance, the porosity of a fibrous porous media can be kept constant whereas other parameters can be changed (see Eq. (1)). Hence, it is necessary to take this point into account in geometrical modelling of such materials for their transport property estimation, which has not been considered by other researchers. In order to do so, we need to have in-depth understanding of these micro structural parameters for each type of GDL. Such data can be measured optically by a microscope or other methods, as discussed in the following sub-sections.

2-1-1. Fiber angle distribution

In [1] model, the angles between fibers are considered the same and equal to zero, which is not realistic. In fact, in each GDL, a distribution of the angles exists, as can be seen in GDL images. These angles can be measured optically for each type of GDL (Fig. 3) and then, their statistical distribution can be obtained, using statistical methods. In a simpler way, especially for the cases where a discrete rather than a continuous random variable exists, a discrete statistical distribution with any arbitrary increment can be used.

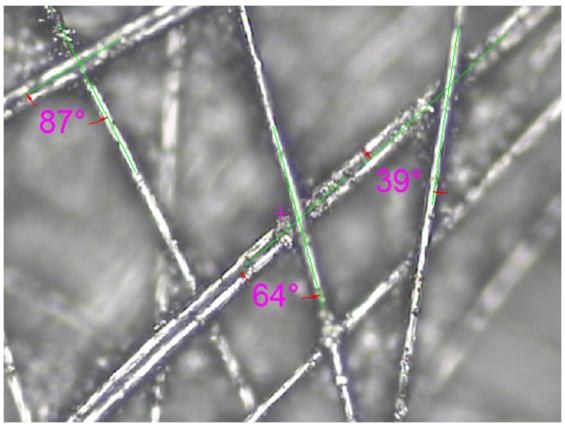

Fig. 3: Angles between fibers measured optically

In this study, the angle distribution for two well-known GDLs Toray and Sigracet have been optically measured, as shown respectively in Figs. 4a and 4b. As seen in these two figures, the majority of the angles tend to take values close to 0° (θ=0; orthogonal arrangement) and the possibility of occurring an angle more than 70° is low, especially for the SGL GDL. The average value of angles obtained for these Toray and SGL GDLs are also shown in Figs. 4 a and b.

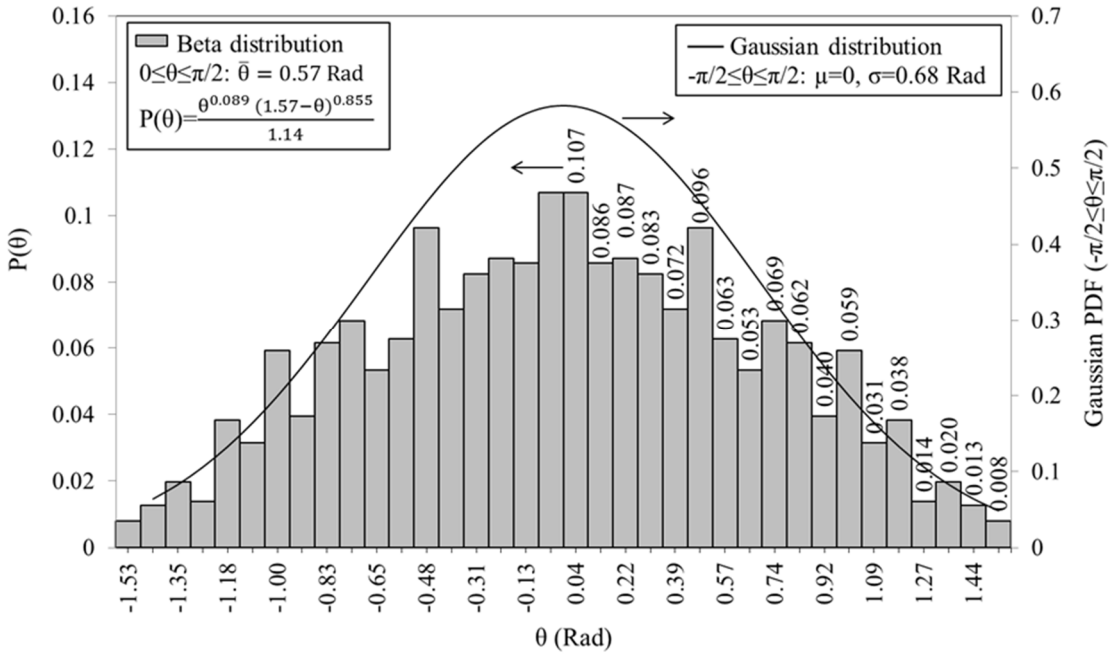

Fig. 4a: Angle distribution of Toray TGP-060

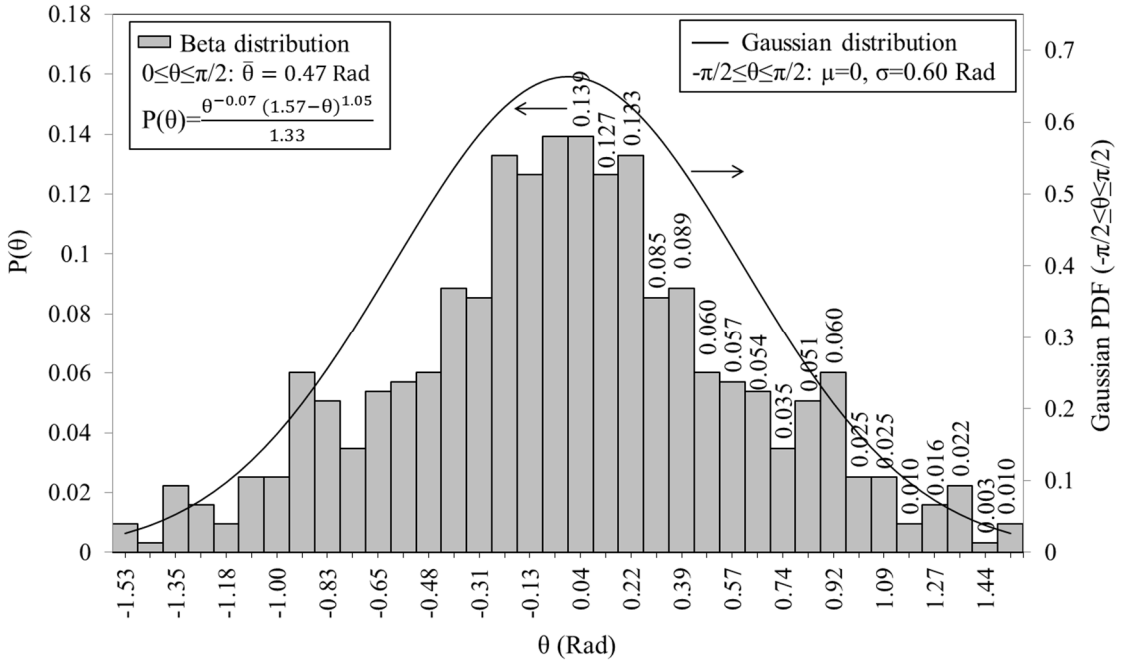

Fig. 4b: Angle distribution of SGL 25BC

The statistical distribution of the fibre angles for each GDL has been calculated by the statistical software Easyfit [17]. As can be observed, the data can be modeled by a Gaussian distribution in a –π/2-π/2 scale and/or a Beta distribution in a 0-π/2 scale for Toray GDL (Fig. 4a). A similar, but not exactly the same, trend can be seen for Sigracet GDL (Fig. 4b). Note that, in general, the angles between two fibers in two neighbouring layers can take any value from 0 to 9o°, yet Figs. 4 a and b can be shown in a –π/2-π/2 scale by considering the supplementary angles, which was resulted in a Gaussian distribution in this scale.

In any case, after measuring the angles, the main question that remains to be answered is how to apply this large number of angle data to the model. Based on a work carried out by Bahrami *et. al.* [18] on the pressure drop of rough micro-tubes, a correction factor or deviations from the average of the angles is introduced. In fact, from the measured angles (the obtained statistical distribution), the average value ($\bar{\theta}$) and also the statistical distribution of the deviations from the average value ($p=\theta-\bar{\theta}$) can be obtained. For each quantity, such as effective thermal conductivity, the correction factor shows the deviation of that quantity from its average value and can be calculated using:

$$M^* = \frac{M_{cor}}{M_{ref}} = \frac{\int_a^b M(\bar{\theta}+p)F(p)dp}{M(\bar{\theta})} \qquad (22)$$

where M is an arbitrary quantity, M_{ref} and M_{cor} are respectively the reference and corrected values of M, and *F(p)* is the statistical distribution of variable p ($a \le p \le b$), obtained from the measured angles.

The corrected values of each quantity (M_{cor}) can also be calculated by

$$M_{cor} = \sum_{i=1}^{N} M(\theta_i)P(\theta_i) \qquad (23)$$

where $P(\theta_i)$ represents the probability of occurring an angle with the value of θ_i and N is the number of the measured angles.

2-1-2. Aspect ratio

The distance between fibers or aspect ratio affects the heat transfer paths and also the number of contact points between adjacent layers of fibres in a fibrous porous media, and therefore, should have a noticeable effect on thermal conductivity. However, to the authors' best knowledge, this important parameter has been overlooked in the existing heat transfer analyses on fibrous porous media. All the previous works carried out on unit cell approach, for calculation of either thermal conductivity [1] or permeability [19-20], considered unity aspect ratio (equal distance between fibers in the *x* and *y* directions, see Fig. 5). Here, for the first time, two technics are presented for finding the aspect ratio for each type of GDLs. One is the same method used for measuring the fibre angles, i.e., optical measurements. The other is based on using the average pore diameter of each GDL obtained by Mercury Intrusion Porosimetry (MIP) measurements. The common approach in both technics is to find another relationship

between l and w and then, solve the obtained equation simultaneously with the porosity, Eq. (1), to obtain the values of l and w and, subsequently, their ratio.

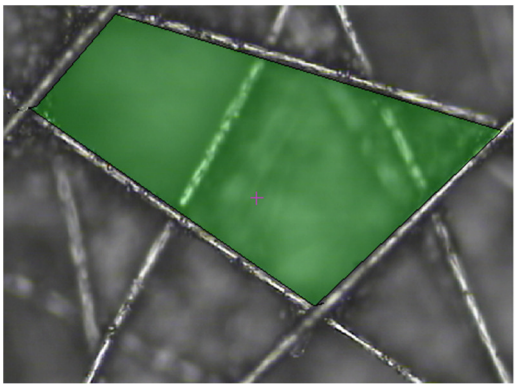

Fig. 5: Measurement of the gap area between fibers for optical measurement of aspect ratio

- Optical measurement of aspect ratio

A sufficient number of areas enclosed between different fibers that are in two neighboring layers (see Fig. 5) can be measured optically, and their average ($A_{ave,m} = \sum_{i=1}^{N_A} A_i / N_A$) can be considered equal to the gap area between fibers in two neighboring layers:

$$A_{ave,m} = (l - d)(w - d) \tag{24}$$

- Aspect ratio determination from MIP data

For many of the commonly used GDLs, such as the ones considered in this study, the pore diameter size has been previously reported in the literature for permeability or other porous media calculations. In general, the pore volume in the unit cell should be the same as the average of the pore volumes inside a GDL, which can be obtained from the MIP method. Considering circular cross-section for the pore openings in the MIP method [21-22], the following relationship between the distance between fibers in the x and y directions, l and w, exists:

$$\frac{\pi d_{p,ave}^2}{4} = (lw\varepsilon) \tag{25}$$

In any case, knowing the porosity and solving this equation, or Eq. (24), simultaneously with the porosity equation of the unit cell, Eq. (1), gives the two unknown variables l and w, and therefore, their ratio. The values of the aspect ratio for some well-known GDLs, obtained from the MIP data [23-27] and optical measurements, are listed in Table 2.

Table 2: Aspect ratios and some relevant specifications for the studied GDLs

	Porosity (-)	Average Pore diameter (μm)	Aspect ratio (-)	
GDL			MIP	Optical
Toray 060	0.78 ±1	39 [23]	3.9	-
Toray 090	0.78 ±1	33 [24]	2.8	-
Toray 120	0.78 ±1	28 [25-26]	2	2.8
SGL 25BC	0.80	42 [27]	4.5	4.1

It is worthwhile to mention that each of these two methods has its own advantages and drawbacks. For instance, the MIP method gives the pore diameter based on volumetric measurements (pores in all the layers) whereas the other works based on gap area measurements in some upper and lower layers (close to sides). However, the MIP method use circular cross-section assumption for the gap area, which cannot be very accurate. Meanwhile, for the case of treated GDLs, the contact angle between mercury and carbon fibers is different that with PTFE and/or MPL. As a result, it may be concluded that for treated thin GDLs, such as most of the Sigracet ones, the optical technic can be more accurate.

2-1-3. Fiber diameter

The diameter of fibers can be optically measured as well and a statistical distribution can also be given for this geometrical parameter. However, there is no need to perform these measurements. This is due to the fact that considering an average value for fiber diameter is sufficient for thermal conductivity modeling, to be discussed in more details later. The average fiber diameters measured in this study for the GDLs Toray and SGL are 8.5 and 8 μm, respectively.

3- RESULTS AND DISCUSSION

Knowing the geometrical parameters of each GDL and how to apply them to the model, we will be able to calculate the through-plane thermal conductivity. A code was written in MATLAB environment so as to perform parametric studies on each of these geometrical parameters. The parametric studies will shed light on the impact of each geometric parameter on thermal conductivity, which provides a deep insight into establishing manufacturing criteria as well as operative conditions. Because of the resistance component-by-component nature of the unit cell approach, it will not be difficult to add the effect of PTFE and Micro Porous Layer (MPL) (treated GDLs) to the present model in the future. Nevertheless, consideration of such effects requires more information such as the thickness of PTFE on both sides and that of the MPL on the catalyst side of GDLs, which have to be reported by the manufactures. This issue can be taken into account in future research for further improvements. Here we present the results of the parametric studies carried out on each parameter as

graphs of thermal conductivity vs. aspect ratio with varying that parameter for typical porosities. It should be noted that wherever one parameter is changed, the other parameters are kept constant at their initial (actual) values unless mentioned otherwise.

3-1. Fiber angle

As mentioned, each type of GDL has its own micro structure, thus a different fiber angle distribution. By plugging the angle statistical distribution (0-π/2 scale) into the correction factor relation, Eq. (22), one can calculate the thermal conductivity corrected based on the angle distribution. In a simpler way, independent of the type of the obtained statistical distribution, the average thermal conductivity can be estimated by Eq. (23).

- Thermal resistance correction factors

From the angle distribution, one can find the average value (see Figs. 4a and 4b) and also the correction factors for deviation of all the possible angles from this average. The values of the correction factors for thermal resistance components of each GDL have been given in Table 3. Note that the correction factors for gas resistances of the top block are always unity, since they are not dependent on fiber angle, see Eqs. (14) and (15) in Table 1, and therefore, were not given in Table 3. As seen in Table 3, the gas thermal resistance correction factor R_{gc2}, unlike all the other gas resistances, is far from unity and therefore, seems to be the most sensitive with respect to angle distribution. Finally, the most important (controlling) factors are related to the spreading/constriction resistances, which are close to unity. In fact, these correction factors show the deviation of each angle from the average value for each GDL. It should be noted that the gas resistances are so large (compare to other resistances) that the heat prefers to pass through the solid almost exclusively, even by experiencing another large resistance (spreading/constriction resistance) that is still much less than the gas resistances themselves. As a result, the gas thermal resistances do not have any significant impact on the through-plane thermal conductivity compared to the solid resistances.

Table 3: Typical values of correction factors for thermal resistance components of each GDL

	Thermal resistance correction factors			
GDL	R^*_{sp}	$R^*_{g,2}$	$R^*_{gc,2}$	R^*_{tot}
Toray 060	1.06	0.94	1.41	1.03
SGL 25BC	1.12	0.95	1.49	1.09

- Thermal resistance and thermal conductivity dependency on fiber angles

The angle between two fibers determines the area of the contact spot, which, in fact, affects the thermal contact resistance considered as spreading/constriction resistance. The dependency of the ratio of spreading/constriction to the total resistance has been shown in Fig. 6. As can be observed, the dependency is not simple and the contribution of the spreading/constriction resistance is always more than 50%, which indicates the importance of this resistance compared to the other ones.

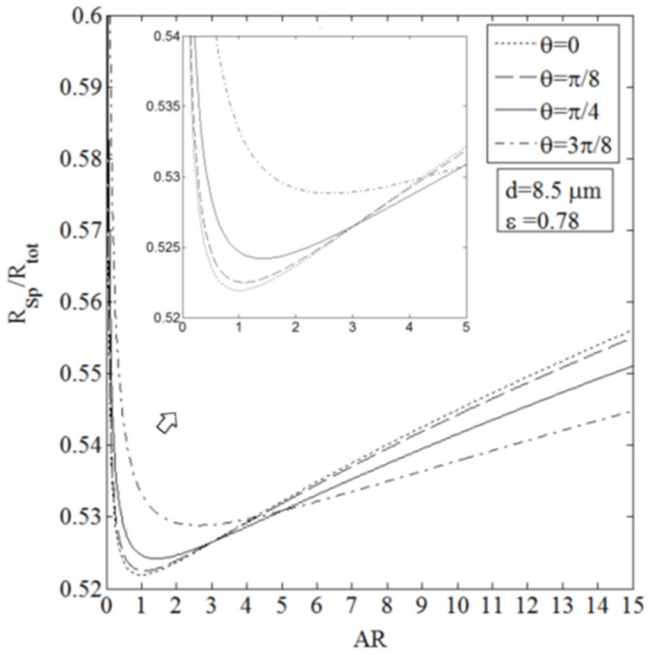

Fig. 6: Dependency of spreading/constriction resistance on angle in GDLs

Figure 7 depicts the dependency of the thermal conductivity on fiber angle at different aspect ratios, which shows more complex dependencies compared to Fig. 6, as there is no specific trend at the typical range of aspect ratios, i.e., the values between 1 and 7. For instance, for the aspect ratios between 1 and 3, the thermal conductivity decreases with angle; whereas for the values between 4 and 5, the thermal conductivity increases. For aspect ratios higher than 8, any increase in angle will result in an increase in thermal conductivity, which shows a completely different behaviour compared to the values of aspect ratios near to unity. As mentioned, the spreading/constriction resistance has the most contributions to the total thermal resistance, especially at higher aspect ratios (compared to unity). At aspect ratios close to unity at which the thermal conductivity is maximum, the spreading/constriction resistance has its lowest contributions.

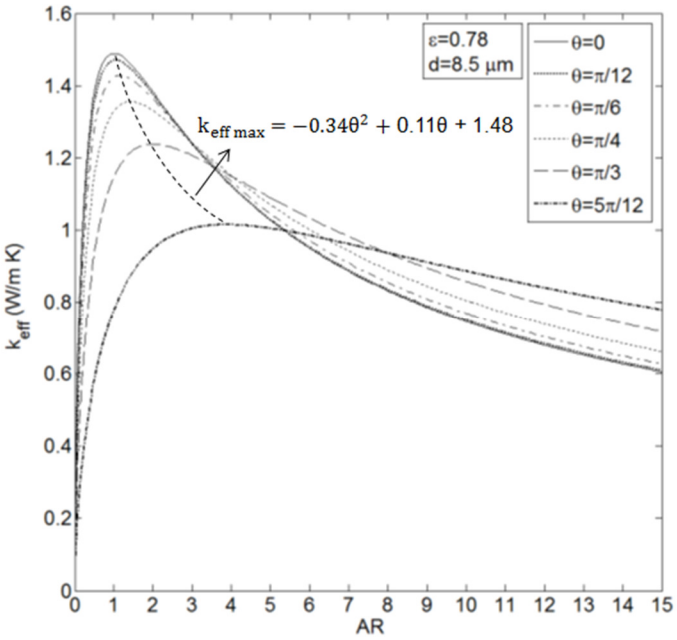

Fig. 7: Dependency of thermal conductivity on angle in GDLs

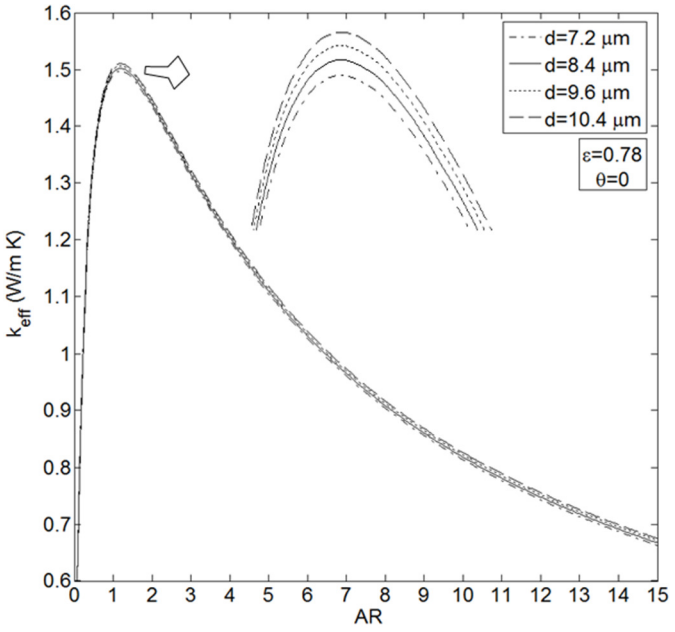

Fig. 8: Effect of diameter on through-plane thermal conductivity in GDLs

Another interesting and important point to notice with respect to manufacturing process is related to the maximum value of thermal conductivity occurring at zero angle (θ=0), which corresponds to the orthogonal arrangement of fibers. If we connect the maximum points and then, correlate the maximum effective thermal conductivity in terms of the fiber angle (θ) (for a specified porosity and diameter), a relatively simple expression can be found, as shown in the figure. This indicates that the dependency of the *maximum* thermal conductivity on fiber angles is not complex, especially for the typical fiber angles ($0 \le \theta \le \pi/3$). Similar studies on the in-plane and electrical conductivity as well as permeability can be useful to find the final best fiber angle for GDLs.

3-2. Fiber diameter

The changes in thermal conductivity for different fiber diameters are shown in Fig. 8 at different aspect ratios. As it can be seen, the thermal conductivity is almost independent of fiber diameter for any value of porosity or aspect ratio. This conclusion contains an important point that the fiber diameter can be manipulated for increasing other transport properties such as permeability without any reduction in through-plane thermal conductivity.

3-3. Aspect ratio

One of the most important geometrical parameters of fibrous porous materials is the aspect ratio. This parameter can usually be as important and effective as porosity, as it can be manipulated for getting the best transport properties for different purposes. Figure 9 represents the thermal conductivity as a function of two important parameters, aspect ratio and porosity. As can be observed from this figure, the dependency of thermal conductivity on porosity is not as complex as angle. Figure 9, similar to Fig. 8, depicts a maximum at an aspect ratio very close, but not necessarily equal, to unity, for each value of porosity. At specified values of θ and d (real case), interestingly enough, the maximum thermal conductivity, $k_{\text{eff max}}$, is practically independent of the aspect ratio. This can be very important for GDL manufacturing. For each type of GDL with different porosities, on the other hand, d and θ are usually fixed, and as a result, it will be accurate to account for $k_{\text{eff max}}$ as a function of porosity only; i.e., $k_{\text{eff max}} = f(\varepsilon)$. Therefore, it is sufficient to, one time, determine or measure the aspect ratio for each type of GDLs and subsequently, determine the optimum relationship. Connecting the maximum points in the cases shown in Fig. 9, a *linear* equation is obtained in the form of:

$$k_{\text{eff max}} = -8.48\varepsilon + c \qquad (26)$$

where c is a constant number at each θ (and d) (e.g., if θ =0 (d=8.5 μm); then c=8.13). In general, the dependency of the maximum thermal conductivity on porosity is linear and much more than that on other geometrical parameters. For the typical

range of fibers angles in GDLs, that is, $0 \le \theta \le \pi/3$ (see Figs. 4 a and b), the maximum thermal conductivity is practically independent of aspect ratio (Fig. 7, also see Figs. 8 and 9). As a result, $k_{\text{eff max}}$ can be considered as a function of only two geometrical parameters, ε and θ.

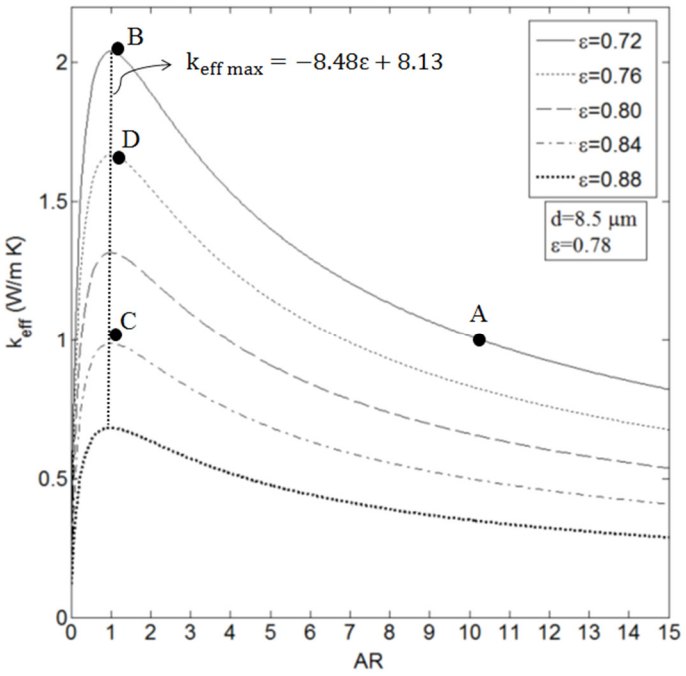

Fig. 9: Effect of aspect ratio on through-plane thermal conductivity at different porosities in GDLs

It should be noted that the unity value of the aspect ratio corresponds to the square arrangement, being the best aspect ratio for having the highest through-plane thermal conductivity. However, other transport properties such as in-plane thermal conductivity, permeability, and electrical conductivity have to be considered. As a result, an optimization of these properties with respect to the geometrical parameters is ultimately required to determine an optimum structure of a GDL for better water and heat management of fuel cells, which would be the purpose of our future research.

Figure 9 can also be very helpful to illustrate the importance of the aspect ratio in comparison to the most important parameter of a porous media, i.e., porosity. It is obvious that with increasing the porosity (at fixed values of aspect ratio and angle), the thermal conductivity decreases whereas the permeability increases. As a result, there is a trade-off between the through-plane thermal conductivity and permeability in terms of porosity. For instance, consider points A, B, C, and D on Fig. 9. To increase the thermal conductivity from 1 to 2 and, in fact, make it double, the first idea that usually comes to mind is to decrease the porosity (e.g., from 0.8 to 0.72, shown in Fig. 9), which may significantly decrease other transport properties such as permeability. However, based on the results of this study, we can double the thermal conductivity from point A to point B by only manipulating the aspect ratio and keep the porosity fixed (ε=0.72). As a result, one could be able to double the thermal conductivity without decreasing the porosity.

As another example, we can keep the through-plane thermal conductivity fixed and increase the porosity or decrease aspect ratio by following any horizontal straight line on Fig. 9 (e.g., from point A to point C). In general, depending on the specific application and the targeted properties, one can keep one or two of the geometrical parameters fixed and change the others to reach an optimum structure of the fibrous media. These points can be considered as some important criteria for manufacturing of GDLs to optimize their microstructures as much as possible for better water and heat management.

Finally, we consider points A and D where point D has a higher thermal conductivity with more porosity. From this, it can be concluded that a fibrous pours media with higher porosity will not have necessarily a lower thermal conductivity. This surprising conclusion contradicts the traditional notion, i.e., the more the porosity, the less the solid, and therefore, the less the thermal conductivity, on which all the available models have been based. As a result, development of the models for estimation of the thermal conductivity of a fibrous media as a function of only solid and pore fractions (e.g., asymptotic solutions and/or Boltzmann methods) may not be useful without considering this point. In general, the important points discussed here can assist developing new approaches to fibrous porous media, from the viewpoint of manufacturing process to that of transport property estimation and modelling.

3-4. Model verification

The results of the present model will be compared with that of Sadeghi *et al.* [1] and also to experimental data [28-31]. Different kinds of well-known GDLs with known through-plane thermal conductivity (Toray TGP-H-060 to 120 and SGL 25BC) have been chosen and then their thermal conductivities were calculated using both models.

As can be seen from Fig. 10, the both models could have very good predictions of the thermal conductivity of the untreated Toray GDLs (TGP H-060 and TGP H-090). Note that in [28] the thermal conductivities were not measured at vacuum conditions (even though some insulation have been used), which was resulted in a little over-measurement, as pointed out by [28] authors. Another point to notice is that the thermal conductivities measured in [28] have been obtained from the so-called two-thickness method for TGP-H-060 and TGP-H-090. According to Table 2, the porosities of these two GDLs are the same and their aspect ratios are close to each other. As a result, the only value of the thermal conductivity obtained for both GDLs TGP-H-060 and -090 by using the two-thickness method can be considered as the average value of their actual thermal conductivities.

We also implemented both models at another temperature, 73 °C, for which one experimental data is also available for verification. For this temperature as well, both models predicted the data reasonably well. Since there is no data for Toray at 56 °C where the experimental data for some Sigracet GDLs is available, we calculated the thermal conductivity by both models at this temperature and then compare the obtained result with the average of the experimental data reported at 25 and 73 °C. For this temperature as well, both models, especially the model of [1], show good agreements. From these comparisons, one can conclude that both models account for the effect of temperature on effective thermal conductivity.

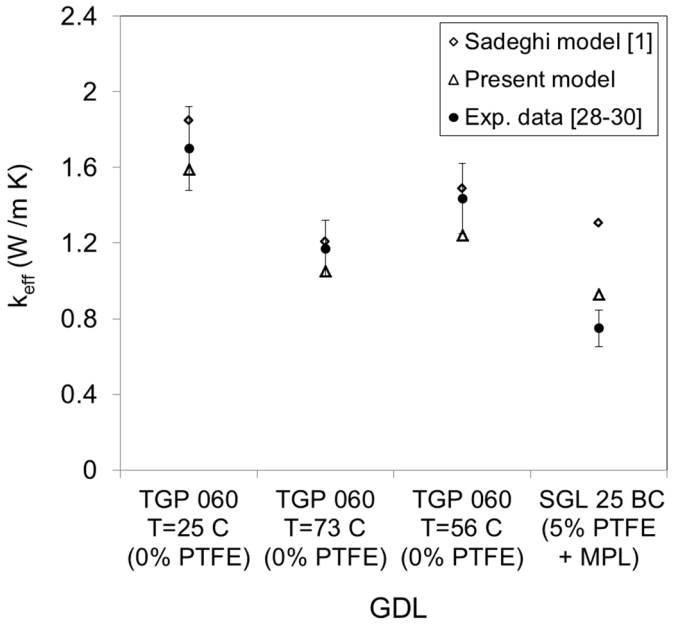

Fig. 10: Comparison of the thermal conductivities calculated by the models with experimental data

Some experimental data measured at different conditions have been reported in [31] for each of treated Torays TGP-H-060, 090, and 120 (5% PTFE), separately (Table 4). In estimation of the thermal conductivity, the [31] authors assumed a negligible thermal contact resistance between two samples (also see [32]) based on the observed little changes in the sample-sample contact resistance with increasing the compression pressure. However, from the independency of the contact resistance on compression pressure, it cannot be concluded that this resistance is negligible or zero. Nevertheless, the data of [31] can still be used for the purpose of qualitative comparisons between the considered Torays, since a common term (resistance) has been neglected in all the measurements. As can be observed from Table 4, the measured data show a reduction in thermal conductivity from TGP-H-120 to TGP-H-060 at all the compression loads. This interesting reduction trend can now be explained by the effect of the aspect ratio parameter, as with increasing this ratio from TGP-H-120 to TGP-H-060 (see Table 2), the effective thermal conductivity decreases. This trend cannot be explained or considered by all the available models including Sadeghi *et. al.* model.

Table 4: Experimental data of [31] for evaluation of the aspect ratio effect on thermal conductivity in different Torays

	$k_{\text{eff}}(W/m\,K)$		
	Compression pressure (Bar)		
Type of Toray	4.6	9.3	13.9
TGP-H-060	0.41	0.53	0.66
TGP-H-090	0.50	0.65	0.73
TGP-H-120	0.62	0.81	0.89

Finally, we consider SGL 25 BC to further investigate the effect of geometrical parameters on thermal conductivity. Although the PTFE and MPL effects have not yet been considered in the model, some qualitative comparisons can be still made by considering the fact that the PTFE and MPL reduction effect on thermal conductivity is not much based on experimental evidence (see, e.g., Refs. [26] and [30]). As can be seen in Fig. 10, the models have completely different predictions of the thermal conductivity of this GDL. The present (statistical) model could estimate the thermal conductivity much better than the [1] model that highly overpredicted the thermal conductivity because of considering unity aspect ratio and zero value of angle (orthogonal arrangement of fibers).

4- CONCLUSION

In this paper, a statistical unit cell model was proposed for estimation of the through-plane thermal conductivity of GDLs, which considers not only porosity, but also other geometrical issues such as angle distribution and aspect ratio parameter. The geometrical parameters of a GDL structure, their effect on through-plane thermal conductivity, and how to measure or determine them for different types of GDL were discussed in detail. These parameters have been measured (or reported) for some widely-used GDLs such as Toray and Sigracet. The parameter of the aspect ratio was discussed and found to be as important and effective as porosity in conduction heat transfer.

It was also illustrated, for the first time in this paper, that the traditional thought, i.e., a fibrous porous media with higher porosity has a lower thermal conductivity, cannot always be correct. In other words, it is possible for two fibrous media with the same porosity to have completely different thermal conductivity due to the contributions of other geometrical parameters, especially aspect ratio. Based on this important point, the difference in thermal conductivities of the different types of Toray having the same porosity could be explained and analyzed. The best structure of a GDL for maximum through-plane thermal conductivity was also obtained. It was also concluded that the *maximum* thermal conductivity is not practically a function of fiber diameter and aspect ratio, and only dependent on porosity and fiber angle. In general, the geometrical concepts and the measured data presented in this paper can be useful for GDL manufacturing as well as for estimation of other transport properties such as permeability.

ACKNOWLEDGMENTS

The Natural Sciences and Engineering Research Council of Canada (NSERC) for financial support of this work is acknowledged.

REFERENCES

[1] E., Sadeghi, M., Bahrami, N., Djilali, Analytic determination of the effective thermal conductivity of PEM fuel cell gas diffusion layers, Journal of Power Sources 179 (2008) 200–208.

[2] J.B., Chaitanya, T.T., Stefan, Effect of anisotropic thermal conductivity of the GDL and current collector rib width on two-phase transport in a PEM fuel cell, Journal of Power Sources 179 (2008) 240–251.

[3] P., Andreas, V., Damien, S., Frank, T., Georgio, X-ray computed tomography of gas diffusion layers of PEM fuel cells: Calculation of thermal conductivity, International Journal of Hydrogen Energy 35 (2010) 3751–3757.

[4] E., Sadeghi, M., Bahrami, N., Djilali, Effective thermal conductivity and thermal contact resistance of gas diffusion layers in PEM fuel cells. Part 1: Effects of compressive load, Journal of Power Sources, 196 (2011) 246-254.

[5] E., Sadeghi, M., Bahrami, N., Djilali, Effective thermal conductivity and thermal contact resistance of gas diffusion layers in PEM fuel cells. Part 2: Hysteresis Effect under Cyclic Compressive Load, Journal of Power Sources, 195 (2010) 8104-8109.

[6] E., Sadeghi, M., Bahrami, N., Djilali, A novel approach to determine the in-plane thermal conductivity of gas diffusion layers in proton exchange membrane fuel cells, Journal of Power Sources, 196 (2011) 3565-3571.

[7] M.F., Mathias, J., Roth, J., Fleming, W., Lehnert, Diffusion media materials and characterisation. In: W., Vielstich, H.A., Gasteiger, A., Lamm. editors. Handbook of fuel cells: fundamentals, technology and applications. John Wiley; 2003.

[8] M., Wang, J.H., He, J.Y., Yu, N., Pan, Lattice Boltzmann modeling of the effective thermal conductivity for fibrous materials, International Journal of Thermal Science, 46 (9) (2007) 848–855.

[9] J., Ramousse, S., Didierjean, P., Lottin, D., Maillet, Estimation of the effective thermal conductivity of carbon felts used as PEMFC Gas Diffusion Layers, International Journal of Thermal science, 47 (2008) 1–8.

[10] A., Pfrang, D., Veyret, F., Sieker, Tsotridis, G., X-ray computed tomography of gas diffusion layers of PEM fuel cells: Calculation of thermal conductivity, International Journal of Hydrogen Energy, 35 (2010) 3751-3757.

[11] M., Bahrami, M.M., Yovanovich, J.R., Culham, Effective thermal conductivity of rough spherical packed beds, International Journal of Heat Mass Transfer 49 (2006) 3691–3701.

[12] M., Bahrami, J.R., Culham, M.M., Yovanovich, Schneider, G.E., Review of thermal joint resistance models for non-conforming rough surfaces, ASME Journal of Applied Mechanics Review, 59 (2006) 1–12.

[13] M., Bahrami, M.M., Yovanovich, J.R., Culham, J.R., A compact model for contact of rough spheres, ASME Journal of Tribology, 127 (2005) 884–889.

[14] M., Bahrami, M.M., Yovanovich, J.R., Culham, Thermal joint resistance of non-conforming rough surfaces with gas-filled gaps, Journal of Thermophysics and Heat Transfer, 18 (2004) 326–332.

[15] M., Bahrami, J.R., Culham, M.M., Yovanovich, Thermal contact resistance: a scale analysis approach, ASME Journal of Heat Transfer 126 (6) (2004) 896–905.

[16] M., Bahrami, M.M., Yovanovich, J.R., Culham, Thermal contact resistance at low contact pressure: effect of elastic deformation, International Journal of Heat and Mass Transfer, 48 (16) (2005) 3284-3293.

[17] Easyfit software, MathWave Technology, http://www.mathwave.com/help/easyfit/index.html.

[18] Bahrami, M., Yovanovich, M.M., Culham, J.R., Pressure drop of laminar, fully developed flow in rough microtubes, ASME J. of Fluid Engineering, 128 (2006) 632-637.

[19] A., Tamayol, M., Bahrami, Analytical determination of viscous permeability of fibrous porous media, International Journal of Heat and Mass Transfer 52 (2009) 2407–2414

[20] J.T., Gostick, M.W., Fowler, M.D., Pritzker, M.A., Ioannidis, L.M., Behra, In-Plane and Through-Plane Gas Permeability of Carbon Fiber Electrode Backing Layers, Journal of Power Sources, 162 (2006) 228–238.

[21] P.A., Webb, An introduction to the physical characterization of materials by mercury intrusion porosimetry with emphasis on reduction and presentation of experimental data, Micromeritics Instrument Corporation, Norcross, Georgia, 2001.

[22] H.L., Ritter, L.C., Drake, Pore-size distribution in porous materials. Pressure porosimeter and determination of

complete macropore-size distribution, Industrial and Engineering Chemistry, 17 (1945) 782–786.

[23] M., Mathias, J., Roth, J., Fleming, W., Lehnert, Diffusion Media Materials and Characterization," Handbook of Fuel Cells—Fundamentals, Technology and Applications, Vol. 3, Vielstich, W., Gasteiger, H. and A. Lamm, editors., Wiley, New York, Chap. 46 (2003).

[24] A., El-kharouf, B.G., Polleta, D., Brettb, Effect of commercial gas diffusion layer (gdl) properties on pemfc performance – from ex-situ testing to modelling, www.fuelcells.bham.ac.uk.

[25] V., Radhakrishnan, P., Haridoss, Effect of cyclic compression on structure and properties of a Gas Diffusion Layer used in PEM fuel cells, International Journal of Hydrogen Energy, 35 (2010) 11107-11118.

[26] J., Gostick, M., Pritzker, M., Ioannidis, M., Fowler, Impact of liquid water on reactant mass transfer in PEM fuel cell electrodes, Journal of the Electrochemical Society 157 (2010) B563-B571.

[27] Z., Lu, M.M., Daino, C., Rath, S.G., Kandlikar, Water management studies in PEM fuel cells, part III: Dynamic breakthrough and intermittent drainage characteristics from GDLs with and without MPLs, International Journal of Hydrogen Energy 35 (2010) 4222-4233.

[28] M., Khandelwal, M.M., Mench, Direct measurement of through-plane thermal conductivity and contact resistance in fuel cell materials, Journal of Power Sources 161 (2006) 1106–1115.

[29] Toray carbon paper-Manufacturer data sheet, http://www.torayca.com/index2.html.

[30] A., Radhakrishnan, Thermal conductivity measurement of gas diffusion layer used in PEMFC, PhD thesis, Rochester Institute of Technology, New York, USA (2009).

[31] O., Burheim, J.G., Pharoah, H., Lampert, P.J.S., Vie, S., Kjelstrup, Through-plane Thermal Conductivity of PEMFC Porous Transport Layers, ASME Journal of fuel Cell Science and Technology, 8 (2011) doi: 10.1115/1.4002403.

[32] O., Burheim, P.J.S., Vie, J.G., Pharoah, S., Kjelstrup, Ex situ measurements of through-plane thermal conductivities in a polymer electrolyte fuel cell, Journal of Power sources 195 (2010) 249-256.